SUV39H1/H3K9me3 attenuates sulforaphane-induced apoptotic signaling in PC3 prostate cancer cells

Citation	Watson, G. W., Wickramasekara, S., Palomera-Sanchez, Z., Black, C., Maier, C. S., Williams, D. E., ... & Ho, E. (2014). SUV39H1/H3K9me3 attenuates sulforaphane-induced apoptotic signaling in PC3 prostate cancer cells. Oncogenesis, 3, e131. doi:10.1038/oncsis.2014.47
DOI	10.1038/oncsis.2014.47
Publisher	Nature Publishing Group
Version	Version of Record
Terms of Use	http://cdss.library.oregonstate.edu/sa-termsofuse

OPEN

Citation: Oncogenesis (2014) **3**, e131; doi:10.1038/oncsis.2014.47

www.nature.com/oncsis

ORIGINAL ARTICLE

SUV39H1/H3K9me3 attenuates sulforaphane-induced apoptotic signaling in PC3 prostate cancer cells

GW Watson[1,2], S Wickramasekara[3], Z Palomera-Sanchez[2], C Black[2], CS Maier[3], DE Williams[4,5], RH Dashwood[4,6] and E Ho[1,2,5]

The isothiocyanate sulforaphane is a promising molecule for development as a therapeutic agent for patients with metastatic prostate cancer. Sulforaphane induces apoptosis in advanced prostate cancer cells, slows disease progression *in vivo* and is well tolerated at pharmacological doses. However, the underlying mechanism(s) responsible for cancer suppression remain to be fully elucidated. In this investigation we demonstrate that sulforaphane induces posttranslational modification of histone methyltransferase SUV39H1 in metastatic, androgen receptor-negative PC3 prostate cancer cells. Sulforaphane stimulates ubiquitination and acetylation of SUV39H1 within a C-terminal nuclear localization signal peptide motif and coincides with its dissociation from chromatin and a decrease in global trimethyl-histone H3 lysine 9 (H3K9me3) levels. Exogenous SUV39H1 expression leads to an increase in H3K9me3 and decreases sulforaphane-induced apoptotic signaling. SUV39H1 is thus identified as a novel mediator of sulforaphane cytotoxicity in PC3 cells. Our results also suggest SUV39H1 dynamics as a new therapeutic target in advanced prostate cancers.

Oncogenesis (2014) **3,** e131; doi:10.1038/oncsis.2014.47; published online 8 December 2014

INTRODUCTION

Prostate cancer is one of the most commonly diagnosed cancers in the United States, the incidence of which is expected to increase as the population ages. Several treatment strategies have been developed for prostate cancer therapy, including surgical removal of the prostate, radiation therapy, hormone or androgen deprivation therapy and chemotherapy. A majority of cases initially respond to frontline treatments; however, despite best efforts, resistant clones arise to resume growth and seed distal sites with metastatic tumors.[1] Once this occurs, survival rates decrease dramatically and treatment options are limited.

Sulforaphane (1-isothiocyanato-4-methylsulfinylbutane) is an isothiocyanate derived from cruciferous vegetables that is known to possess cancer-suppressive activity.[2] The compound is well tolerated and is cytotoxic specifically toward transformed cells, inducing cell cycle arrest and apoptosis. Although differences in sensitivity between cell lines do exist, the tissue of origin or genetic profile does not appear to be determinant: sulforaphane is cytotoxic to many human cancer cell lines *in vitro*, including prostate,[3] breast,[4] ovarian,[5,6] colon[7] and pancreatic cancers,[8] and can suppress cancer progression in genetic models of colon[9] and prostate[10] carcinoma. Sulforaphane has been shown to (i) induce cell death in metastatic prostate cancer cell lines while sparing primary prostate epithelial cells,[3] (ii) decrease metastases in a genetically engineered mouse model of prostate cancer[10] and (iii) is not associated with adverse effects when administered at pharmacological doses in rodents.[11] These observations make sulforaphane a compound of interest for development as a prostate cancer therapeutic agent.

Several investigations have characterized broad alterations in the epigenome in prostate cancer patients and suggested that epigenetic profile and expression levels of chromatin-modifying enzymes (CMEs) have some prognostic value.[12–15] Progressive dysregulation of the epigenome as cells adopt a malignant phenotype is now recognized as an active contributor to transformation that works in tandem with genetic alterations to allow cancer progression. As epigenetic state is reversible, targeting the epigenome is an attractive therapeutic strategy. Indeed, a number of small molecule inhibitors targeting CMEs are approved or are in clinical and preclinical trials as chemotherapeutic agents.[16] Recent investigations characterizing sulforaphane-induced changes in the level and activity of CMEs has led to the hypothesis that modulation of these enzymes contributes to cell cycle arrest and apoptosis in prostate cancer cells. Sulforaphane leads to a decrease in global histone deacetylase (HDAC) activity in prostate cancer cells through depletion of specific HDAC isoforms.[3] Sulforaphane has also been shown to decrease DNA methyltransferase (DNMT) levels in prostate cancer cells.[17] Little is known concerning the effects of sulforaphane on histone methylation—only one investigation has characterized an influence on histone H3 lysine 27 trimethylation (Balasubramanian *et al.*[18])—despite the fact that DNMT, HDAC and histone methyltransferases (HMT) and demethylases (HDM) physically interact and work cooperatively in larger protein complexes to maintain or alter chromatin structure.[19–21] Furthermore, any postulated heterochromatin-dependent contribution of HDAC or DNMT depletion is likely secondary to changes in histone methylation, as DNMT functions downstream of HMTs and HDAC

[1]Department of Molecular and Cellular Biology, Oregon State University, Corvallis, OR, USA; [2]College of Public Health and Human Sciences, Oregon State University, Corvallis, OR, USA; [3]Department of Chemistry, Oregon State University, Corvallis, OR, USA; [4]Department of Environmental and Molecular Toxicology, Oregon State University, Corvallis, OR, USA; [5]Linus Pauling Institute, Oregon State University, Corvallis, OR, USA and [6]Center for Epigenetics and Disease Prevention, Texas A&M Health Science Center, Houston, TX, USA. Correspondence: Dr E Ho, Moore Family Center, School of Biological and Population Health Sciences, Oregon State University, Milam Hall Room Number 103, Corvallis, OR 97331, USA.
E-mail: Emily.Ho@oregonstate.edu
Received 29 July 2014; revised 26 September 2014; accepted 15 October 2014

enzymes lack protein domains that can independently recognize chromatin.[22–24] This led us to investigate whether changes in global histone methylation accompany changes in CME protein level and activity in sulforaphane-treated prostate cancer cells. As HDAC and DNMT enzymes facilitate heterochromatin formation and stabilization, and sulforaphane depletes these proteins in prostate cancer cells, we hypothesized a decrease in histone methyl marks associated with heterochromatin in sulforaphane-treated prostate cancer cells.

Histone methylation is more complex than the chromatin marks controlled by HDAC (acetylation) and DNMT (DNA methylation) enzymes. As opposed to existing in one of two states, each with a characteristic association with chromatin structure, the outcome of histone methylation is residue- and mark-specific (see Martin and Zhang[25] and references therein for summary). We focused our investigation on the archetypal heterochromatin mark trimethyl-histone H3 lysine 9 (H3K9me3) and conducted our mechanistic investigation in PC3 cells, a culture model of metastatic, aggressive, androgen receptor-negative prostate cancer. PC3 cells are an advantageous prostate cancer cell line to test our hypothesis, because sulforaphane depletes HDAC[3] and DNMT[17] enzymes in these cells and the H3K9me3 mark is controlled by one HMT, SUV39H1, with no functional redundancy.[26] Here we present evidence supporting a model where a decrease in H3K9me3 mediated by posttranslational regulation of SUV39H1 enhances apoptotic signaling in PC3 cells in response to sulforaphane, suggesting indirect inhibition or destabilization of SUV39H1 as a potential treatment strategy.

RESULTS

Sulforaphane decreases global trimethyl H3K9 levels

Sulforaphane treatment leads to a global decrease in H3K9me3 in PC3 cells (Figure 1). The decrease was detectable as early as 6 h post treatment and remained at a depressed level through 12 h. At 24 h, H3K9me3 returned to control levels (not shown). An assessment of H3K9me3 level in sulforaphane-treated LNCaP and DU145 metastatic prostate cancer cell lines showed no global response (not shown).

Sulforaphane has previously been shown to induce G2/M arrest in PC3 cells,[27] and H3K9me3 levels have recently been found to fluctuate with the cell cycle, increasing at the centromere through metaphase before reaching a peak and declining through anaphase.[28] The global decrease in H3K9me3 we observed following sulforaphane treatment suggests that large blocks of chromatin, possibly megabases in length, are undergoing H3K9me3 depletion, which would be consistent with alterations in centromeric H3K9me3 levels. This raises the possibility that a global decrease in H3K9me3 in sulforaphane-treated cells is an artifact of cell cycle arrest and not depletion of heterochromatic CMEs *per se*. Cyclin B1 protein level was therefore analyzed to assess the possibility of a cell cycle effect. An analysis of cyclin B1 protein level (Supplementary Figure 1), known to accumulate in metaphase-arrested PC3 cells,[29] showed no difference between treatment groups within our treatment period of interest, suggesting the decrease in H3K9me3 is independent of cell cycle and not a consequence of arrest. Visualization of 4,6-diamidino-2-phenylindole (DAPI)-stained sulforaphane-treated nuclei also indicated arrest before metaphase (not shown).

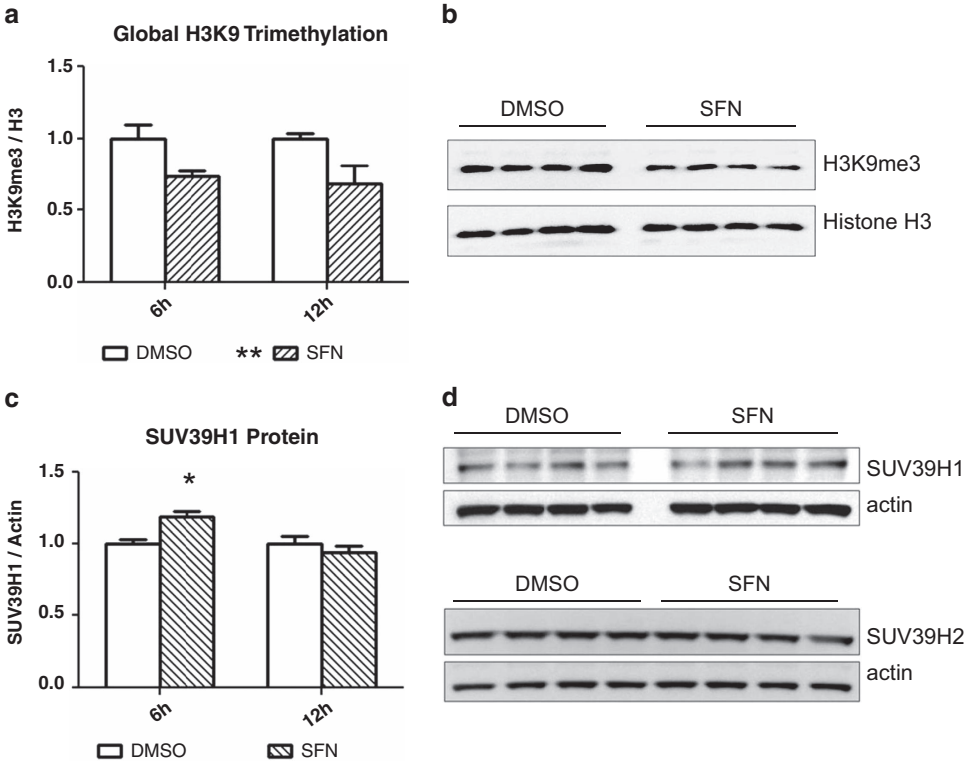

Figure 1. (**a**) Sulforaphane causes a global decrease in H3K9-trimethylation in PC3 cells. H3K9me3 was decreased relative to global histone H3 at 6 and 12 h post treatment ($P < 0.01$ by two-way analysis of variance (ANOVA) with Bonferroni post test, mean+s.e.m. for three independent experiments). (**b**) Representative blot from one of three independent experiments at 12 h post treatment. (**c**) SUV39H1 is increased at 6 h post treatment ($P < 0.05$ by two-way ANOVA with Bonferroni post test, mean+s.e.m. for three independent experiments). The early increase in SUV39H1 was not maintained, with the protein returning to control level by 12 h. (**d**) Representative blots from one of three independent experiments at 12 h post treatment. β-Actin was probed as a loading control. SFN, sulforaphane.

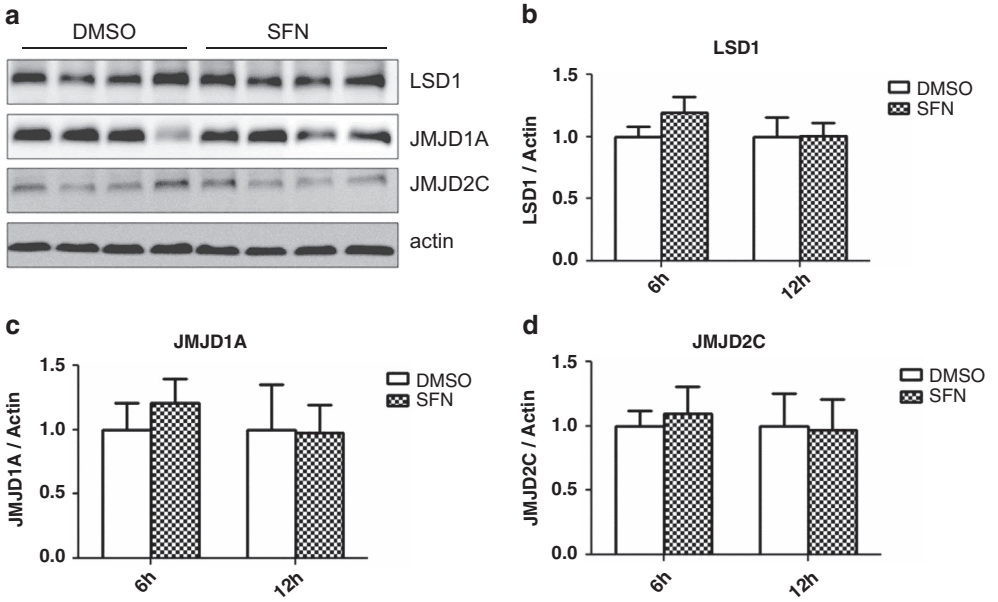

Figure 2. (**a**) Sulforaphane does not significantly alter the global level of selected H3K9 demethylases, although the expression is highly variable in PC3 cells (12 h blot pictured). No change in (**b**) LSD1 (KDM1A), (**c**) JMJD1A (KDM3A) or (**d**) JMJD2C (KDM4C) was noted in sulforaphane-treated cells (two-way analysis of variance with Bonferroni post test, mean+s.d.). SFN, sulforaphane.

Sulforaphane does not affect the protein level of H3K9 methyl modifiers

H3K9 methylation is controlled by multiple HMTs and HDMs, with several enzymes capable of catalyzing specific modifications. A decrease in global H3K9me3 levels could be caused by a decrease in HMT activity, an increase in HDM activity, or some combination of the two. SUV39H methyltransferase proteins (specifically isoform 1) control H3K9me3 at pericentromeric and centromeric chromatin domains,[30] suggesting depletion or inactivation of SUV39H1 could account for the global decrease in H3K9me3 we observed by western blotting. Furthermore, targeted knockdown of SUV39H1 by small interfering RNA in PC3 cells leads to a global decrease in H3K9me3 and has a minimal effect on global gene expression,[26] suggesting SUV39H1 is solely responsible for H3K9 trimethylation with little or no functional redundancy and that SUV39H1-specific effects are independent of gene promoter regulation. We observed a transient increase in SUV39H1 in sulforaphane-treated cells and no change in SUV39H2 protein level over the treatment period (Figure 1).

HDM enzymes are a relatively recent discovery and less is known about their role in genome maintenance; we nevertheless assessed the protein level of several HDMs known to have activity toward H3K9 (Kondo[31]). No significant increase in the level of HDM LSD1 (KDM1A), JMJD1A (KDM3A) or JMJD2C (KDM4C) was maintained over the 12-h treatment period (Figure 2).

No sustained change in the protein level of the enzymes that control H3K9 methylation suggests regulation through a post-translational mechanism. We focused our investigation on SUV39H1, as it can influence global H3K9me3 and is known to physically interact with HDAC and DNMT enzymes.[32,33] We hypothesized an increase in posttranslational modifications associated with decreased SUV39H1 activity or stability in response to sulforaphane.

Sulforaphane leads to SUV39H1 posttranslational modification

SUV39H1 is known to be regulated posttranslationally: the protein is subject to phosphorylation,[30] acetylation,[34] ubiquitination[35] and methylation,[36] all of which have been associated with changes in localization or decreased stability and activity. Discrete lysine residues on SUV39H1 have been characterized as subject to posttranslational modification. Acetylation of lysine 266 has been shown to inhibit catalytic activity[34] and ubiquitination of lysine 87 has been shown to facilitate degradation.[35] We used liquid chromatography-coupled tandem mass spectrometry (LC-MS/MS) to assess sulforaphane-induced posttranslational modifications of endogenous SUV39H1 protein in PC3 cells (Figure 3 and Supplementary Figure 2). We identified ubiquitinated (ub-K393-SUV39H1) and acetylated SUV39H1 (ac-K394-SUV39H1) only in sulforaphane-treated cells on an overlapping C-terminal peptide (379-MDSNFGLAGLPGSPKKRVR-397). Ubiquitinated SUV39H1 (ub-SUV39H1) was confirmed by immunoprecipitation (Figure 4). Increased ub-SUV39H1 occurred despite a global decrease in ubiquitinated proteins.

Sirtuin 1 (SirT1) is reported to control SUV39H1 ubiquitination and acetylation,[35] suggesting SUV39H1 modification may be the result of sulforaphane-induced changes in the protein level or activity of SirT1. Sulforaphane has been found to influence the protein level of some Sirtuins in colon cancer cells.[37] We did not observe a hypothesized decrease in SirT1 protein level that would explain SUV39H1 destabilization or inhibition in sulforaphane-treated PC3 cells (Figure 5). A test of direct inhibition of SirT1 catalytic activity by the intracellular metabolites of sulforaphane at relevant intracellular concentration[3,38,39] also revealed no activity as a direct inhibitor (Figure 5). These data suggest SirT1-independent posttranslational control of SUV39H1 protein.

Sulforaphane leads to a decrease in chromatin-associated SUV39H1

The effects of lysine 393 or 394 modification are not known, but these residues fall within a predicted nuclear localization signal peptide motif (391-SPKKRVRIE-399) (predicted by three independent motif recognition tools;[40–42] Supplementary Figure 3). This led us to hypothesize that modification of these residues would be associated with a change in SUV39H1 localization. Visualization by immunofluorescence revealed discrete nuclear foci characteristic of chromatin-associated SUV39H1. A separate pool of mobile SUV39H1 was also identified in the perinuclear cytoplasmic region and spread diffusely within the nucleus (Figure 6c). Quantification

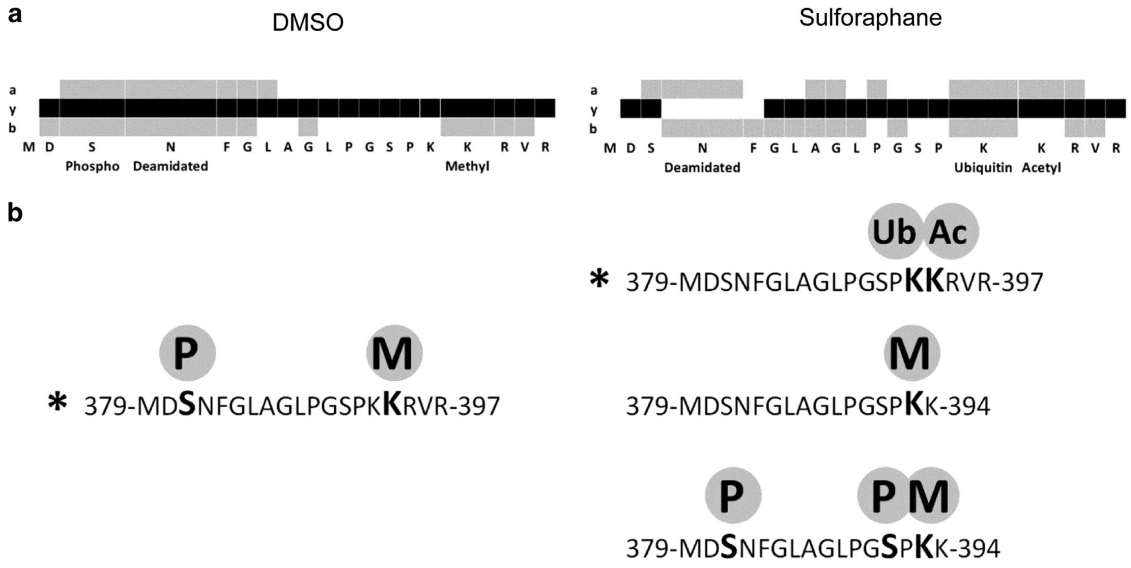

Figure 3. Identification of ubiquitinated and acetylated lysine residues on SUV39H1 in sulforaphane-treated PC3 cells. (**a**) a, y and b ion peptide coverage by liquid chromatography–tandem mass spectrometry (LC-MS/MS) of the C-terminal peptide 379-MDSNFGLAGLPGSPKKRVR-397 in control-treated (dimethyl sulfoxide (DMSO)) (left) and sulforaphane-treated (right) cell lysate. Coverage corresponds to asterisked peptides in **b**. (**b**) Peptides and modifications of the C-terminal region. The C-terminal region of interest is phosphorylated (P) and methylated (M) in both DMSO control and sulforaphane-treated lysates. Ubiquitinated (Ub) and acetylated (Ac) lysines were only identified in sulforaphane-treated cells. Spectra for the asterisked peptides in **b** can be found in Supplementary Figure 2.

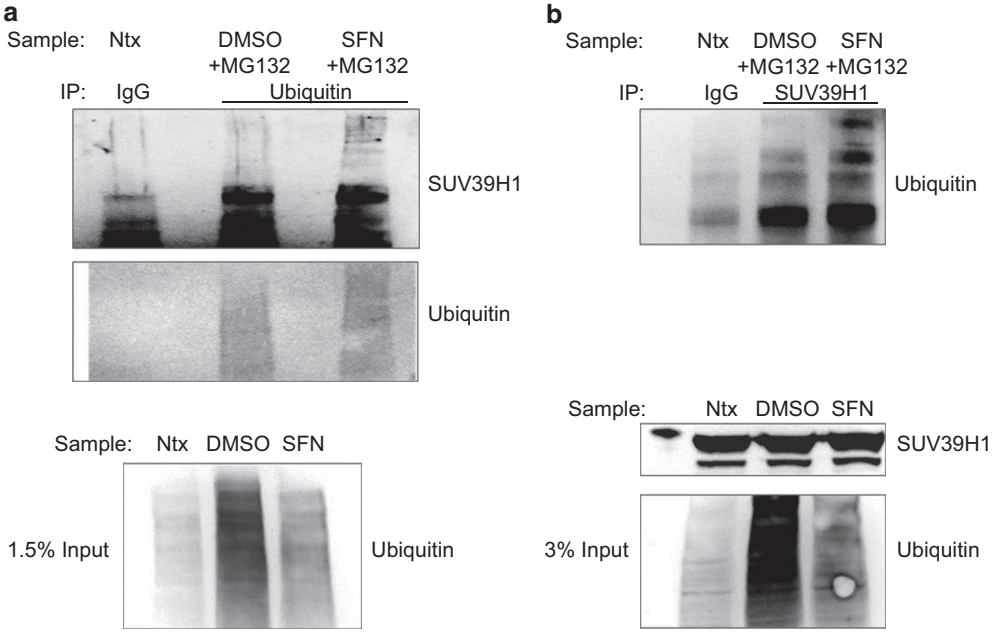

Figure 4. (**a**) PC3 cells were co-treated with MG132 (10 μM) and dimethyl sulfoxide (DMSO) or sulforaphane for 9 h. Ubiquitinated proteins were immunoprecipitated from lysates and subsequently analyzed for SUV39H1 protein. An increase in ubiquitinated SUV39H1 was noted in sulforaphane-treated cells. The increase in high-molecular weight SUV39H1 occurred despite a global decrease in ubiquitinated protein levels. Untreated PC3 lysate (Ntx) was immunoprecipitated with normal IgG and analyzed in parallel as a control. (**b**) The reverse immunoprecipitation (SUV39H1 immunoprecipitation → ubiquitin analysis) under the same experimental conditions as in **a** confirmed increased ubiquitinated SUV39H1 in sulforaphane-treated cells. SFN, sulforaphane.

by western blotting showed an increase in cytoplasmic (or mobile) SUV39H1 and a decrease in nuclear (or immobile, histone associated) SUV39H1 in sulforaphane-treated cells (Figure 6).

Exogenous expression of SUV39H1 decreases sulforaphane-induced apoptotic signaling

SUV39H1 modification, altered localization and decreased global H3K9me3 levels in sulforaphane-treated PC3 cells suggests that SUV39H1 and/or H3K9me3 depletion may have a role in sulforaphane-induced cytotoxicity.[3,43] To test whether SUV39H1 or global H3K9me3 contribute to sulforaphane-triggered apoptosis in PC3 cells, we overexpressed SUV39H1 by transient transfection to increase H3K9me3, then treated with sulforaphane and monitored cleaved poly-ADP ribose polymerase—a terminal cleavage event in apoptotic signaling—to assess changes in cytotoxicity (Figure 7 and Supplementary Figure 4). Exogenous

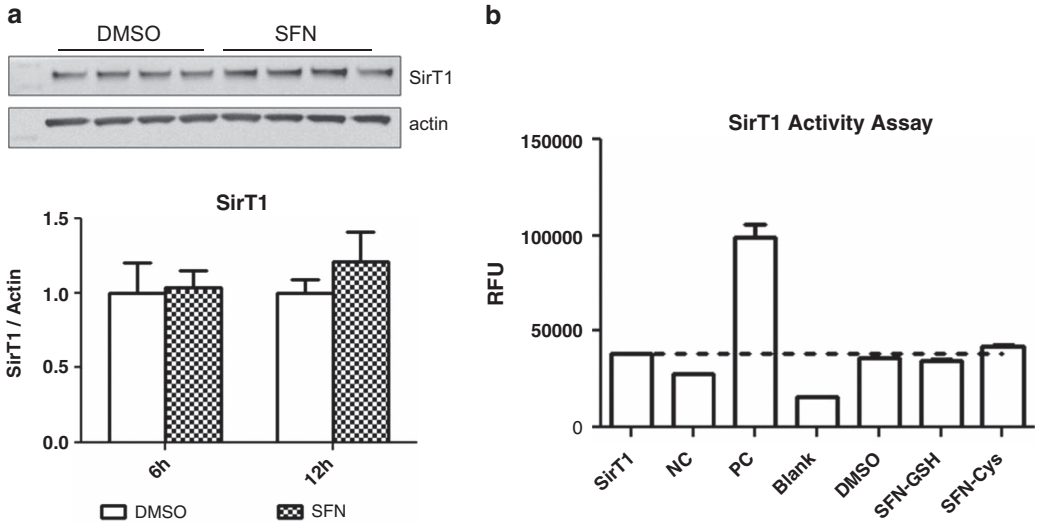

Figure 5. (**a**) Sulforaphane does not affect SirT1 protein level at 6 or 12 h post treatment. Sample blot from 12-h time point pictured (two-way analysis of variance with Bonferroni post test, mean+s.d.). (**b**) Intracellular sulforaphane metabolites do not directly inhibit or activate SirT1 catalytic activity (Student's *t*-test, mean+s.d.). RFU, relative fluorescence units; Sirt1, basal enzyme activity; NC, negative control (nicotinamide solution); PC, positive control (resveratrol); Blank, no enzyme; SFN-GSH, sulforaphane-glutathione (1 mM); SFN-Cys, sulforaphane-cysteine (150 μM).

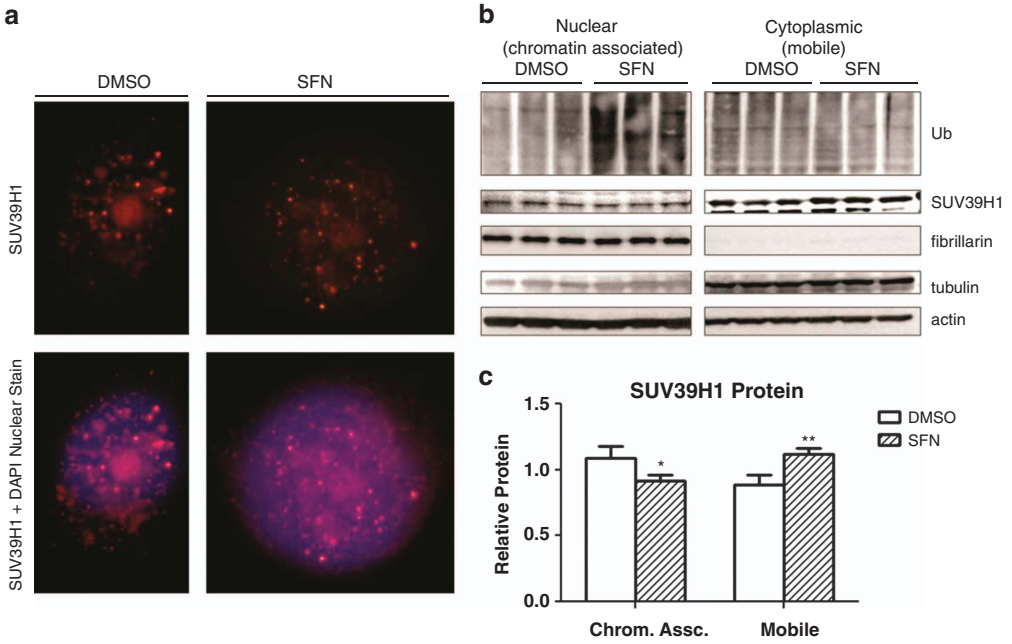

Figure 6. (**a**) Representative image of control (dimethyl sulfoxide (DMSO)) and sulforaphane-treated (12 h) PC3 cells with nuclear (4,6-diamidino-2-phenylindole (DAPI)) and SUV39H1 labeling for immunofluorescent imaging. The chromatin-associated SUV39H1 foci and dispersed nuclear and perinuclear mobile fractions are readily visible. (**b**) Sulforaphane leads to a decrease in chromatin-associated SUV39H1. PC3 cells were treated for 8 h with sulforaphane. MG132 was spiked into the culture dishes at a final concentration of 50 μM for the last 2 h of the treatment. The high-dose, short-duration treatment was to halt a sulforaphane-stimulated increase in proteasome activity and decrease the impact of any MG132 toxicity. The experimental conditions did inhibit protein degradation (increase in ubiquitinated proteins in sulforaphane-treated PC3 cells). (**c**) Densitometry showed a decrease in histone-associated SUV39H1 and an increase in mobile SUV39H1 (*$P < 0.05$, **$P < 0.01$ by two-way analysis of variance with Bonferroni post test, mean+s.d.). Histone-associated (nuclear, immobile) SUV39H1 normalized to nuclear marker fibrillarin. Mobile (cytoplasmic) SUV39H1 normalized to β-actin. SFN, sulforaphane.

SUV39H1 expression (SUV) increased global H3K9me3 levels relative to control (GFP (green fluorescent protein)) and sulforaphane did stimulate apoptotic signaling as measured by cleaved poly-ADP ribose polymerase. We noted a decrease in cleaved poly-ADP ribose polymerase in SUV39H1-overexpressing cells in response to sulforaphane relative to GFP-control, suggesting SUV39H1/H3K9me3 is protective against sulforaphane-induced cytotoxicity and that a global decrease in H3K9me3 contributes to cell death in PC3 cells.

DISCUSSION

In this investigation we characterized a novel response to the natural compound sulforaphane in PC3 prostate cancer cells

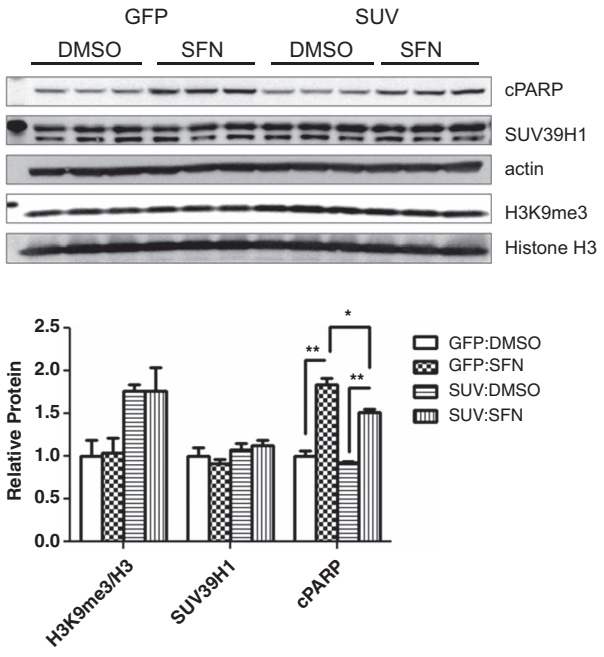

Figure 7. SUV39H1 decreases cleaved poly-ADP ribose polymerase (cPARP) in sulforaphane-treated PC3 cells. PC3 cells were transfected with GFP (control) or SUV39H1 (SUV) expression vector and allowed to recover for 36 h. Cells were incubated with sulforaphane for 24 h before collecting whole-cell lysates. H3K9me3 is increased in SUV39H1-transfected PC3 cells (SUV: dimethyl sulfoxide (DMSO), SUV:SFN) relative to GFP control (GFP:DMSO, GFP:SFN) (normalized to histone H3), although no increase in total SUV39H1 protein was noted (normalized to β-actin). Sulforaphane treatment significantly increased apoptotic signaling as assessed by cPARP in GFP- and SUV39H1-transfected cells. SUV39H1 overexpression significantly decreased cPARP protein levels, indicating decreased apoptotic signaling (*$P < 0.05$, **$P < 0.01$ by one-way analysis of variance with Bonferroni post test for each protein, mean+s.e.m. for two independent experiments; blot from representative experiment pictured).

involving the histone modifier SUV39H1. We present evidence supporting a model where sulforaphane-induced posttranslational modification of SUV39H1 decreases the chromatin-associated cellular fraction, leading to a decrease in H3K9me3 (Figures 1, 3, 4 and 6). We go on to show that SUV39H1/H3K9me3 decreases apoptotic signaling in PC3 cells (Figure 7), suggesting the changes in SUV39H1 dynamics in sulforaphane-treated PC3 cells contribute to cytotoxicity. Taken together, these results suggest that posttranslational modification of SUV39H1 may be a promising therapeutic strategy in the treatment of advanced prostate cancer.

Perturbations in SUV39H1 protein level in normal cells is known to increase cancer risk: engineered mice that are SUV39H-null show an increased susceptibility to cancer[44] and mice that overexpress SUV39H1 show defects in cell differentiation and proliferation that can result in chronic myeloid leukemia.[45] SUV39H1 can also influence metastatic potential in transformed cells: a potentially chromatin-independent role for SUV39H1 in facilitating cell motility and invasion has recently been characterized in hepatocellular carcinoma cells.[46] SUV39H1 knockdown specifically in PC3 cells also supports a gene expression-independent role in cell proliferation.[26] Chemotherapeutic strategies pursuing direct SUV39H1 inhibition are being investigated, although the *in vivo* activity of the leading candidate, chaetocin, is debatable.[47–50] Our data suggests an alternative strategy for targeting SUV39H1 involving indirect destabilization or modulation of the posttranslational modifiers that regulate SUV39H1, several of which have been characterized.[34,35] Small molecule modulators are currently being tested that target such proteins (for example, MDM2 inhibitors[51]), yet the contribution, if any, of SUV39H1-modification to the activity of these molecules is not known. Assessing this possible contribution will be important to gain a complete understanding of how and why such molecules are effective agents.

Although sulforaphane is known to induce cellular stress and general protein turnover through the ubiquitin-proteasome pathway[52] and induction of the autophagic pathway,[53] the data presented here suggests that sulforaphane leads to directed SUV39H1 modification in PC3 cells. We observed an increase in ubiquitinated SUV39H1, despite a global decrease in ubiquitinated proteins in sulforaphane-treated cells (Figure 4), suggesting controlled regulation as opposed to general turnover. We also noted no significant increase in SUV39H1 protein level in SUV39H1-overexpressing PC3 cells, despite a global increase in H3K9me3 (Figure 7). The finding that global H3K9me3 levels are not affected in sulforaphane-treated LNCaP and DU145 cells also suggests directed regulation in response to sulforaphane in PC3 cells. Further work will be needed to identify the factors accounting for the differential response between cell lines and will be important in developing a genetic signature of the subset of advanced prostate cancers that would be susceptible to exploiting modulation of SUV39H1 dynamics to enhance apoptotic signaling.

An increase in global H3K9me3 levels in SUV39H1-transfected cells with no corresponding increase in SUV39H1 protein level (Figure 7) suggests SUV39H1 protein level is tightly regulated in PC3 cells through posttranslational control, and that SUV39H1 dynamics are what determine global H3K9me3. Taken together with the shift in SUV39H1 pools from chromatin associated to mobile in sulforaphane-treated cells (Figure 6), these data suggest a model where SUV39H1 rate-of-renewal at heterochromatic sites is the parameter affected by sulforaphane-induced modification. The increase in cytoplasmic (or mobile) SUV39H1 should therefore be interpreted as a delayed renewal time at chromatin, which we propose to be a consequence of modification of a conserved nuclear localization signal. An alternative hypothesis could propose decreased enzymatic activity through interference with conserved putative zinc-coordinating cysteines in the adjacent post-SET (Su(var)3-9, Enhancer-of-zeste, Trithorax) domain (Supplementary Figure 3). Mutagenesis studies have shown these cysteines to be required for enzymatic activity in other post-SET domain-containing H3K9 methyltransferases.[54] However, given the rather modest decrease in global H3K9me3 in sulforaphane-treated cells compared with catalytically impaired SUV39H1 mutants,[35,55,56] inhibition of SUV39H1 activity is less likely. This interpretation is also in agreement with a recent report by Park *et al.*[57] where they characterized CDK2-dependent phosphorylation of SUV39H1 at lysine 391, a mark we identified in sulforaphane-treated PC3 lysate by mass spectrometry (Figure 3). Mutagenesis at lysine 391 to mimic phosphorylation did not alter enzymatic activity, but did influence occupancy at heterochromatin and led to a decrease in H3K9me3 at specific repeat elements. This supports our model proposing that modification of this region leads to decreased H3K9me3 through a shift from chromatin-associated to mobile SUV39H1 and not through impaired enzymatic activity.

This is the first investigation to characterize changes in SUV39H1/H3K9me3 in the response to sulforaphane in any cell type. Although SUV39H1 turnover rate and recovery time have been shown to have a significant impact on global H3K9me3 and genome stability,[35] the impact in the context of sulforaphane treatment is not known. We found that increased H3K9me3 in SUV39H1-transfected cells associated with decreased apoptotic signaling (Figure 7), indicating that H3K9me3 is protective in sulforaphane-treated PC3 cells and suggesting that modulation of

this methyl mark and modifier actively contributes to sulforaphane cytotoxicity.

An important aspect of our investigation is the characterization of SUV39H1 modification within 12 h of sulforaphane treatment. Sulforaphane is rapidly metabolized and excreted from the body.[58,59] Even when administered intravenously at a pharmacological dose to achieve ~15 μM plasma concentration in a rat model, the majority of sulforaphane and its metabolites are cleared in less than 12 h.[11] Our treatment periods exist within the pharmacokinetic parameters of sulforaphane metabolism *in vivo*, suggesting our results may be achievable in a clinical setting.

Here we implicated a new chromatin mark and CME in the cellular response to sulforaphane in PC3 prostate cancer cells. We propose a model where sulforaphane causes a decrease in H3K9me3 through posttranslational modification of H3K9 methyltransferase SUV39H1, and that this actively contributes to sulforaphane-induced apoptotic signaling. These findings suggest that targeting SUV39H1 dynamics to enhance cell death signaling may be a strategy worth exploring in treating advanced metastatic cancers.

MATERIALS AND METHODS

Cells and reagents

Prostate cancer cells (PC3 and LNCaP) were purchased from American Type Culture Collection (Manassas, VA, USA) or received as a gift (DU145 line from Dr Philippe T Georgel, Marshall University). Cells were maintained in RPMI-1640 media with L-glutamine supplemented with fetal bovine serum (50 ml fetal bovine serum/500 ml media) at 37 °C 5% CO_2. PC3 and LNCaP cell lines were validated by Idexx Radil (Columbia, MO, USA) on 24 December 2012. Sulforaphane was purchased from LKT Laboratories (St Paul, MN, USA). Sulforaphane-glutathione and sulforaphane-cysteine were purchased from Toronto Research Chemicals (Toronto, ON, Canada). MG132 was purchased from Santa Cruz Biotechnology (Dallas, TX, USA). Primary antibodies against ubiquitin (Santa Cruz Biotechnology), SUV39H2 (Santa Cruz Biotechnology), SUV39H1 (Santa Cruz Biotechnology, Millipore (Billerica, MA, USA)), SirT1 (eBioscience, San Diego, CA, USA), β-actin (Sigma, Saint Louis, MO, USA), trimethyl histone H3 lysine 9 (Millipore), cleaved poly-ADP ribose polymerase (Cell Signaling, Danvers, MA, USA), cyclin B1 (Cell Signaling), fibrillarin (Cell Signaling), LSD1 (Abcam, Cambridge, MA, USA), JMJD1A (Abcam), JMJD2C (Abcam), α-tubulin (Sigma) and histone H3 (Bethyl, Montgomery, TX, USA), and horseradish peroxidase-conjugated secondary antibodies (Santa Cruz) were used in accordance with the manufacturer's protocol. SirT1 Activity Assay was conducted in accordance with the manufacturer's protocol (Sigma). Sulforaphane-cysteine and sulforaphane-glutathione conjugates were produced in house. Liquid chromatography–MS grade solvents were purchased from Millipore. Subconfluent cells were treated with control (dimethyl sulfoxide), sulforaphane (15 μM) and/or MG132 (at the indicated dose) and incubated at 37 °C 5% CO_2 until collection.

Protein analysis

Protein lysates were prepared in RIPA protein lysis buffer (150 mM NaCl, 1% Triton X-100, 0.5% NaDOC, 0.1% SDS, 20 mM Tris pH 8.0) supplemented with protease inhibitor cocktail (Thermo, Waltham, MA, USA) followed by sonication in an ice-cold waterbath. Lysates were cleared by centrifugation at 4 °C and quantitated by DCA Protein Assay (BioRad, Hercules, CA, USA). For SUV39H1 localization, cells were incubated in 0.5% Triton X-100 phosphate-buffered saline with protease inhibitor cocktail for 15 min on ice. Cells were then vortexed and nuclei spun out. Nuclei were washed in phosphate-buffered saline and resuspended in RIPA lysis buffer and incubated on ice for 10 min. Lysates were then subjected to sonication in an ice-cold waterbath.

Proteins were separated by SDS–polyacrylamide gel electrophoresis and blotted to a polyvinylidene difluoride membrane (BioRad) using NuPAGE Reagents and equipment in accordance with the manufacturer's protocols (Invitrogen, Carlsbad, CA, USA). Membranes were blocked and probed for proteins of interest following manufacturer's protocols. Membranes were incubated in SuperSignal West Femto Reagent (Thermo) and developed on the AlphaInnotech FluorChem 8900 system (ProteinSimple, San Jose, CA, USA). Membranes were stripped using ReBlot Plus Strong Solution as needed in accordance with the manufacturer's protocol (Millipore). Densitometric analyses were performed on the native membrane image using AlphaInnotech FluorChem 8900 software. For each membrane, the relative densitometric value of each replicate for a given probe was normalized to the corresponding relative level of the normalizing protein. For graphing, treatments are expressed relative to Control (set to the value 1). Proteins are normalized to β-actin unless otherwise indicated.

Immunoprecipitation

Lysates were prepared by one freeze–thaw in non-denaturing lysis buffer (137 mM NaCl, 1% Triton X-100, 2 mM EDTA, 20 mM Tris pH 8.0), cleared by centrifugation and quantitated by DCA Protein Assay (BioRad). Equal protein lysate (2–3 mg) was incubated with primary antibody (anti-ubiquitin or anti-SUV39H1) overnight at 4 °C, then with Protein A agarose (Sigma) or Protein A/G PLUS agarose (Santa Cruz) for 2–4 h at 4 °C. Immunoprecipitates were washed three to five times in non-denaturing lysis buffer and eluted in 2% SDS TBS (Tris-buffered saline) at room temperature for 15 min.

Immunofluorescence

Immunofluorescence was carried out following standard protocols. Briefly, PC3 cells were grown and treated on glass coverslips. Cells were fixed in 100% methanol and then in 4% paraformaldehyde. Fixed cells were permeabilized in 0.4% Triton X-100 phosphate-buffered saline and blocked in 5% bovine serum albumin 0.1% NP-40 phosphate-buffered saline. Cells were probed with SUV39H1 antibody (Santa Cruz), followed by incubation in anti-rabbit Alexa Fluor-555 (Invitrogen) and finally with 4,6-diamidino-2-phenylindole (Millipore). Coverslips were mounted on glass slides using ProLong Gold Antifade Reagent (Invitrogen) and images captured on a Nikon Eclipse E400 microscope using Nikon NIS-Elements software (Nikon, Tokyo, Japan).

Mass spectrometry

PC3 cells were washed twice in 50 mM sodium bicarbonate and subjected to one freeze–thaw at −80 °C in 50 mM sodium bicarbonate. Liberated proteins were separated from cellular debris by centrifugation at 13 000 r.p.m. for 10 min at 4 °C. Proteins were reduced, alkylated and digested using Trypsin Gold in presence of ProteaseMax surfactant according to the manufacturer's protocols (Promega, Madison, WI, USA).

Liquid chromatography–MS/MS analysis was carried out using a nanoAcquity UPLC system (Waters Corporation, Milford, MA, USA) coupled to an LTQ-FT MS instrument (Thermo Fisher Scientific, San Jose, CA, USA). A binary solvent system consisting of solvent A (water with 0.1% formic acid) and solvent B (acetonitrile with 0.1% formic acid) was used for the analyses. Tryptic peptides (2 μl) were loaded onto a peptide trapping column (Michrom Cap Trap; Bruker Daltonics Inc., Billerica, MA, USA) and separated using a C18 analytical column (Agilent Zorbax 300SB-C18 (Santa Clara, CA, USA), 250 × 0.3 mm, 5 μm). Peptides were trapped and washed with 3% solvent B for 3 min at a flow rate of 5 μl/min. Peptide separation was achieved using a linear gradient from 10% to 30% B at a flow rate of 4 μl/min over 102 min. The LTQ-FT mass spectrometer was controlled by Xcaliber 2.0 (Thermo Fisher Scientific) and operated in data-dependent MS/MS acquisition with MS precursor ion scan, performed in the ion cyclotron resonance (ICR) cell, from 350–2000 *m/z*. Instrument resolving power was set to 100 000 at *m/z* 400, and MS/MS scans were performed by the linear ion trap on the five most abundant doubly or triply charged precursor ions detected in the MS scan.

Thermo RAW data files were processed with Mascot database analysis software (v2.3) (Matrix Science, Boston, MA, USA) within Proteome Discoverer v1.4.0 (Thermo). Data files were searched against the Human protein RefSeq database downloaded from NCBI (http://www.ncbi.nlm.nih.gov/protein) and to an in-house database containing SUV39H1 protein sequence (NP_003164.1) and decoy protein sequences including common contaminants.

The following parameters were used to search the database: the digestion enzyme was set to Trypsin and three missed cleavage sites were allowed. The precursor ion mass tolerance was set to 20 p.p.m. and the fragment ion tolerance was set to 1.0 Da. Dynamic modifications that were considered included carbamidomethyl-cysteine (+57.02 Da), oxidated methionine (+15.99 Da), deamidated asparagine or glutamine (+0.98 Da), phospho-serine, -threonine, or -tyrosine (+97.98 Da), ubiquitinated lysine (+114.04 Da), methyl-lysine (+14.02) and acetyl-lysine (+42.01 Da). Automatic target decoy search with 1% false discovery rate was included into the Mascot search. Scaffold_3.3.1 (Proteome Software, Portland, OR, USA)

was used for search data compilation and data evaluation with an embedded X!Tandem database searching algorithm. Protein identifications were accepted if they could be established at >90% probability and contained at least 2 identified peptides per protein with a false discovery rate <5%. Assigned spectra were inspected manually for quality. Spectra assigned to both databases (Human RefSeq and in-house DB) were manually assigned using custom python scripts and the best match selected.

Quantitative real-time PCR

Total RNA was collected by TRIzol reagent in accordance with the manufacturer's protocol (Invitrogen). cDNA was prepared from μg RNA using the SuperScript III kit from Invitrogen. Approximately 50 ng cDNA was amplified by Fast SYBR Green Reagent in accordance with the manufacturer's protocol (Invitrogen) on a 7900HT Real Time PCR Machine (Applied Biosciences, Life Technologies, Carlsbad, CA, USA).

Primers used were as follows: glyceraldehyde 3-phosphate dehydrogenase (sense 5′-CGAGATCCCTCCAAAATCAA-3′, antisense 5′-TTCACACC CATGACGAACAT-3′); HO1 (sense 5′-CTTCTTCACCTTCCCCAAC-3′, antisense 5′-GCTCTGGTCCTTGGTGTCATA-3′); SUV39H1 (sense 5′-GCTAGGCCCGAATG TCGTTA-3′, antisense 5′-GCCTTCTGCACCAGGTAGTT-3′).

SUV39H1 cloning

SUV39H1 coding sequence was amplified from PC3 cDNA using primers to append a 5′ *Eco*RI and 3′ *Not*I restriction site (sense 5′-CTGCCGCC GAATTCCCCGAATGTCGTTAGCCGTGGGGAAAG-3′, antisense 5′-ATCTGAG AGCGGCCGCCACGGCCACAGCCCTGAACG-3′). SUV39H1 coding sequence was digested and ligated into pCMV6-AC-GFP destination vector (Origene, Rockville, MD, USA). The ligation mixture was transformed into One Shot TOP10 Chemically Competent *Escherichia coli* following the manufacturer's protocol (Invitrogen). Plasmid was isolated using the QIAprep Spin Miniprep Kit (Qiagen, Venlo, Netherlands). Candidates were screened for insert using SUV39H1 primers (sense 5′-GCTAGGCCCGAATGTCGTTA-3′, antisense 5′-GCCTTCTGCACCAGGTAGTT-3′) and restriction digest fingerprinting. The final construct selected for PC3 transfection was validated by sequencing at the Center for Genome Research and Bioinformatics at the Oregon State University (sense 5′-GCTAGGCCCGAATGTCGTTA-3′, antisense 5′-GCCTTCTGCACCAGGTAGTT-3′, antisense 5′-ATCTGAGAGCGGCCG CCACGGCCACAGCCCTGAACG-3′). The final construct was found to contain the SUV39H1 RefSeq coding sequence (NM_003173.3).

Transient transfection of PC3 cells

PC3 cells were grown to 70–80% confluence in six-well plates and transfected with pCMV6-AC-GFP or pCMV6-SUV39H1 plasmid using Lipofectamine 2000 according to the manufacturer's recommendations (Invitrogen). Briefly, growth media was replaced with unsupplemented Dulbecco's modified Eagle's medium before transfection. Cells were transfected with 5 μg plasmid per well and allowed to rest for 12 h. Media was then replaced with growth media and cells allowed to recover for 24 h before beginning treatments.

CONFLICT OF INTEREST

The authors declare no conflict of interest.

ACKNOWLEDGEMENTS

This work was supported by the National Institutes of Health (P01CA090890). Oregon State University mass spectrometry facility is supported in part by a grant from the National Institute of Environmental Health Science (P30ES000210).

REFERENCES

1 Karantanos T, Corn PG, Thompson TC. Prostate cancer progression after androgen deprivation therapy: mechanisms of castrate resistance and novel therapeutic approaches. *Oncogene* 2013; **32**: 5501–5511.
2 Juge N, Mithen RF, Traka M. Molecular basis for chemoprevention by sulforaphane: a comprehensive review. *Cell Mol Life Sci* 2007; **64**: 1105–1127.
3 Clarke JD, Hsu A, Yu Z, Dashwood RH, Ho E. Differential effects of sulforaphane on histone deacetylases, cell cycle arrest and apoptosis in normal prostate cells versus hyperplastic and cancerous prostate cells. *Mol Nutr Food Res* 2011; **55**: 999–1009.
4 Pledgie-Tracy A, Sobolewski MD, Davidson NE. Sulforaphane induces cell type-specific apoptosis in human breast cancer cell lines. *Mol Cancer Ther* 2007; **6**: 1013–1021.
5 Chaudhuri D, Orsulic S, Ashok BT. Antiproliferative activity of sulforaphane in Akt-overexpressing ovarian cancer cells. *Mol Cancer Ther* 2007; **6**: 334–345.
6 Chuang LT, Moqattash ST, Gretz HF, Nezhat F, Rahaman J, Chiao JW. Sulforaphane induces growth arrest and apoptosis in human ovarian cancer cells. *Acta Obstet Gynecol Scand* 2007; **86**: 1263–1268.
7 Gamet-Payrastre L, Li P, Lumeau S, Cassar G, Dupont MA, Chevolleau S *et al.* Sulforaphane, a naturally occurring isothiocyanate, induces cell cycle arrest and apoptosis in HT29 human colon cancer cells. *Cancer Res* 2000; **60**: 1426–1433.
8 Pham NA, Jacobberger JW, Schimmer AD, Cao P, Gronda M, Hedley DW. The dietary isothiocyanate sulforaphane targets pathways of apoptosis, cell cycle arrest, and oxidative stress in human pancreatic cancer cells and inhibits tumor growth in severe combined immunodeficient mice. *Mol Cancer Ther* 2004; **3**: 1239–1248.
9 Hu R, Khor TO, Shen G, Jeong WS, Hebbar V, Chen C *et al.* Cancer chemoprevention of intestinal polyposis in ApcMin/+ mice by sulforaphane, a natural product derived from cruciferous vegetable. *Carcinogenesis* 2006; **27**: 2038–2046.
10 Singh SV, Warin R, Xiao D, Powolny AA, Stan SD, Arlotti JA *et al.* Sulforaphane inhibits prostate carcinogenesis and pulmonary metastasis in TRAMP mice in association with increased cytotoxicity of natural killer cells. *Cancer Res* 2009; **69**: 2117–2125.
11 Wang H, Lin W, Shen G, Khor TO, Nomeir AA, Kong AN. Development and validation of an LC-MS-MS method for the simultaneous determination of sulforaphane and its metabolites in rat plasma and its application in pharmacokinetic studies. *J Chromatogr Sci* 2011; **49**: 801–806.
12 Weichert W, Roske A, Gekeler V, Beckers T, Stephan C, Jung K *et al.* Histone deacetylases 1, 2 and 3 are highly expressed in prostate cancer and HDAC2 expression is associated with shorter PSA relapse time after radical prostatectomy. *Br J Cancer* 2008; **98**: 604–610.
13 Ellinger J, Kahl P, von der Gathen J, Rogenhofer S, Heukamp LC, Gutgemann I *et al.* Global levels of histone modifications predict prostate cancer recurrence. *Prostate* 2010; **70**: 61–69.
14 Seligson DB, Horvath S, Shi T, Yu H, Tze S, Grunstein M *et al.* Global histone modification patterns predict risk of prostate cancer recurrence. *Nature* 2005; **435**: 1262–1266.
15 van Leenders GJ, Dukers D, Hessels D, van den Kieboom SW, Hulsbergen CA, Witjes JA *et al.* Polycomb-group oncogenes EZH2, BMI1, and RING1 are overexpressed in prostate cancer with adverse pathologic and clinical features. *Eur Urol* 2007; **52**: 455–463.
16 Kelly TK, De Carvalho DD, Jones PA. Epigenetic modifications as therapeutic targets. *Nat Biotechnol* 2010; **28**: 1069–1078.
17 Hsu A, Wong CP, Yu Z, Williams DE, Dashwood RH, Ho E. Promoter de-methylation of cyclin D2 by sulforaphane in prostate cancer cells. *Clin Epigenet* 2011; **3**: 3.
18 Balasubramanian S, Chew YC, Eckert RL. Sulforaphane suppresses polycomb group protein level via a proteasome-dependent mechanism in skin cancer cells. *Mol Pharmacol* 2011; **80**: 870–878.
19 Bantscheff M, Hopf C, Savitski MM, Dittmann A, Grandi P, Michon AM *et al.* Chemoproteomics profiling of HDAC inhibitors reveals selective targeting of HDAC complexes. *Nat Biotechnol* 2011; **29**: 255–265.
20 Esteve PO, Chin HG, Smallwood A, Feehery GR, Gangisetty O, Karpf AR *et al.* Direct interaction between DNMT1 and G9a coordinates DNA and histone methylation during replication. *Genes Dev* 2006; **20**: 3089–3103.
21 Fritsch L, Robin P, Mathieu JR, Souidi M, Hinaux H, Rougeulle C *et al.* A subset of the histone H3 lysine 9 methyltransferases Suv39h1, G9a, GLP, and SETDB1 participate in a multimeric complex. *Mol Cell* 2010; **37**: 46–56.
22 Cedar H, Bergman Y. Linking DNA methylation and histone modification: patterns and paradigms. *Nat Rev Genet* 2009; **10**: 295–304.
23 Lehnertz B, Ueda Y, Derijck AA, Braunschweig U, Perez-Burgos L, Kubicek S *et al.* Suv39h-mediated histone H3 lysine 9 methylation directs DNA methylation to major satellite repeats at pericentric heterochromatin. *Curr Biol* 2003; **13**: 1192–1200.
24 Vire E, Brenner C, Deplus R, Blanchon L, Fraga M, Didelot C *et al.* The Polycomb group protein EZH2 directly controls DNA methylation. *Nature* 2006; **439**: 871–874.
25 Martin C, Zhang Y. The diverse functions of histone lysine methylation. *Nat Rev Mol Cell Biol* 2005; **6**: 838–849.
26 Kondo Y, Shen L, Ahmed S, Boumber Y, Sekido Y, Haddad BR *et al.* Downregulation of histone H3 lysine 9 methyltransferase G9a induces centrosome disruption and chromosome instability in cancer cells. *PLoS One* 2008; **3**: e2037.
27 Myzak MC, Hardin K, Wang R, Dashwood RH, Ho E. Sulforaphane inhibits histone deacetylase activity in BPH-1, LnCaP and PC-3 prostate epithelial cells. *Carcinogenesis* 2006; **27**: 811–819.

28 Chu L, Zhu T, Liu X, Yu R, Bacanamwo M, Dou Z *et al.* SUV39H1 orchestrates temporal dynamics of centromeric methylation essential for faithful chromosome segregation in mitosis. *J Mol Cell Biol* 2012; **4**: 331–340.
29 Frisa PS, Jacobberger JW. Cell cycle-related cyclin b1 quantification. *PLoS One* 2009; **4**: e7064.
30 Aagaard L, Schmid M, Warburton P, Jenuwein T. Mitotic phosphorylation of SUV39H1, a novel component of active centromeres, coincides with transient accumulation at mammalian centromeres. *J Cell Sci* 2000; **113**(Pt 5): 817–829.
31 Kondo Y. Epigenetic cross-talk between DNA methylation and histone modifications in human cancers. *Yonsei Med J* 2009; **50**: 455–463.
32 Fuks F, Hurd PJ, Deplus R, Kouzarides T. The DNA methyltransferases associate with HP1 and the SUV39H1 histone methyltransferase. *Nucleic Acids Res* 2003; **31**: 2305–2312.
33 Vaute O, Nicolas E, Vandel L, Trouche D. Functional and physical interaction between the histone methyl transferase Suv39H1 and histone deacetylases. *Nucleic Acids Res* 2002; **30**: 475–481.
34 Vaquero A, Scher M, Erdjument-Bromage H, Tempst P, Serrano L, Reinberg D. SIRT1 regulates the histone methyl-transferase SUV39H1 during heterochromatin formation. *Nature* 2007; **450**: 440–444.
35 Bosch-Presegue L, Raurell-Vila H, Marazuela-Duque A, Kane-Goldsmith N, Valle A, Oliver J *et al.* Stabilization of Suv39H1 by SirT1 is part of oxidative stress response and ensures genome protection. *Mol Cell* 2011; **42**: 210–223.
36 Wang D, Zhou J, Liu X, Lu D, Shen C, Du Y *et al.* Methylation of SUV39H1 by SET7/9 results in heterochromatin relaxation and genome instability. *Proc Natl Acad Sci USA* 2013; **110**: 5516–5521.
37 Rajendran P, Kidane AI, Yu TW, Dashwood WM, Bisson WH, Lohr CV *et al.* HDAC turnover, CtIP acetylation and dysregulated DNA damage signaling in colon cancer cells treated with sulforaphane and related dietary isothiocyanates. *Epigenetics* 2013; **8**: 612–623.
38 Ye L, Zhang Y. Total intracellular accumulation levels of dietary isothiocyanates determine their activity in elevation of cellular glutathione and induction of Phase 2 detoxification enzymes. *Carcinogenesis* 2001; **22**: 1987–1992.
39 Zhang Y, Callaway EC. High cellular accumulation of sulphoraphane, a dietary anticarcinogen, is followed by rapid transporter-mediated export as a glutathione conjugate. *Biochem J* 2002; **364**(Pt 1): 301–307.
40 Kosugi S, Hasebe M, Tomita M, Yanagawa H. Systematic identification of cell cycle-dependent yeast nucleocytoplasmic shuttling proteins by prediction of composite motifs. *Proc Natl Acad Sci USA* 2009; **106**: 10171–10176.
41 Lin JR, Hu J. SeqNLS: nuclear localization signal prediction based on frequent pattern mining and linear motif scoring. *PLoS One* 2013; **8**: e76864.
42 Dinkel H, Van Roey K, Michael S, Davey NE, Weatheritt RJ, Born D *et al.* The eukaryotic linear motif resource ELM: 10 years and counting. *Nucleic Acids Res* 2014; **42**: D259–D266.
43 Singh AV, Xiao D, Lew KL, Dhir R, Singh SV. Sulforaphane induces caspase-mediated apoptosis in cultured PC-3 human prostate cancer cells and retards growth of PC-3 xenografts in vivo. *Carcinogenesis* 2004; **25**: 83–90.
44 Peters AH, O'Carroll D, Scherthan H, Mechtler K, Sauer S, Schofer C *et al.* Loss of the Suv39h histone methyltransferases impairs mammalian heterochromatin and genome stability. *Cell* 2001; **107**: 323–337.
45 Czvitkovich S, Sauer S, Peters AH, Deiner E, Wolf A, Laible G *et al.* Over-expression of the SUV39H1 histone methyltransferase induces altered proliferation and differentiation in transgenic mice. *Mech Dev* 2001; **107**: 141–153.
46 Fan DN, Tsang FH, Tam AH, Au SL, Wong CC, Wei L *et al.* Histone lysine methyltransferase, suppressor of variegation 3-9 homolog 1, promotes hepatocellular carcinoma progression and is negatively regulated by microRNA-125b. *Hepatology (Baltimore, MD* 2013; **57**: 637–647.
47 Chaib H, Nebbioso A, Prebet T, Castellano R, Garbit S, Restouin A *et al.* Anti-leukemia activity of chaetocin via death receptor-dependent apoptosis and dual modulation of the histone methyl-transferase SUV39H1. *Leukemia* 2012; **26**: 662–674.
48 Cherblanc FL, Chapman KL, Brown R, Fuchter MJ. Chaetocin is a nonspecific inhibitor of histone lysine methyltransferases. *Nat Chem Biol* 2013; **9**: 136–137.
49 Greiner D, Bonaldi T, Eskeland R, Roemer E, Imhof A. Identification of a specific inhibitor of the histone methyltransferase SU(VAR)3-9. *Nat Chem Biol* 2005; **1**: 143–145.
50 Tibodeau JD, Benson LM, Isham CR, Owen WG, Bible KC. The anticancer agent chaetocin is a competitive substrate and inhibitor of thioredoxin reductase. *Antioxid Redox Signal* 2009; **11**: 1097–1106.
51 Wade M, Li YC, Wahl GM. MDM2, MDMX and p53 in oncogenesis and cancer therapy. *Nat Rev* 2013; **13**: 83–96.
52 Gan N, Wu YC, Brunet M, Garrido C, Chung FL, Dai C *et al.* Sulforaphane activates heat shock response and enhances proteasome activity through up-regulation of Hsp27. *J Biol Chem* 2010; **285**: 35528–35536.
53 Herman-Antosiewicz A, Johnson DE, Singh SV. Sulforaphane causes autophagy to inhibit release of cytochrome C and apoptosis in human prostate cancer cells. *Cancer Res* 2006; **66**: 5828–5835.
54 Zhang X, Tamaru H, Khan SI, Horton JR, Keefe LJ, Selker EU *et al.* Structure of the neurospora SET domain protein DIM-5, a histone H3 lysine methyltransferase. *Cell* 2002; **111**: 117–127.
55 Chin HG, Patnaik D, Esteve PO, Jacobsen SE, Pradhan S. Catalytic properties and kinetic mechanism of human recombinant Lys-9 histone H3 methyltransferase SUV39H1: participation of the chromodomain in enzymatic catalysis. *Biochemistry.* 2006; **45**: 3272–3284.
56 Rea S, Eisenhaber F, O'Carroll D, Strahl BD, Sun ZW, Schmid M *et al.* Regulation of chromatin structure by site-specific histone H3 methyltransferases. *Nature* 2000; **406**: 593–599.
57 Park SH, Yu SE, Chai YG, Jang YK. CDK2-dependent phosphorylation of Suv39H1 is involved in control of heterochromatin replication during cell cycle progression. *Nucleic Acids Res* 2014; **42**: 6196–6207.
58 Hanlon N, Coldham N, Gielbert A, Sauer MJ, Ioannides C. Repeated intake of broccoli does not lead to higher plasma levels of sulforaphane in human volunteers. *Cancer Lett* 2009; **284**: 15–20.
59 Clarke JD, Hsu A, Riedl K, Bella D, Schwartz SJ, Stevens JF *et al.* Bioavailability and inter-conversion of sulforaphane and erucin in human subjects consuming broccoli sprouts or broccoli supplement in a cross-over study design. *Pharmacol Res* 2011; **64**: 456–463.

Supplementary Information accompanies this paper on the Oncogenesis website (http://www.nature.com/oncsis)